Physical and Functional Interactions between PML and MDM2

THE JOURNAL OF BIOLOGICAL CHEMISTRY
Vol. 278, No. 31, Issue of August 1, pp. 29288–29297, 2003

Printed in U.S.A.

Physical and Functional Interactions between PML and MDM2*

Received for publication, December 2, 2002, and in revised form, May 14, 2003
Published, JBC Papers in Press, May 19, 2003, DOI 10.1074/jbc.M212215200

Xiaolong Wei‡, Zhong Kang Yu‡, Arivudainambi Ramalingam‡, Steven R. Grossman§¶‡‡, Jiang H. Yu‖, Donald B. Bloch‖, and Carl G. Maki‡**

From the ‡Department of Radiation Oncology, The University of Chicago, Chicago, Illinois 60637, the §Departments of Adult Oncology and Cancer Biology, Dana Farber Cancer Institute and the ¶Department of Medicine, Brigham and Women's Hospital, Boston, Massachusetts 02115, and the ‖Center for Immunology and Inflammatory Diseases, Department of Medicine, Harvard Medical School and Massachusetts General Hospital, Boston, Massachusetts 02114

The tumor suppressor protein PML and oncoprotein MDM2 have opposing effects on p53. PML stimulates p53 activity by recruiting it to nuclear foci termed PML nuclear bodies. In contrast, MDM2 inhibits p53 by promoting its degradation. To date, neither a physical nor functional relationship between PML and MDM2 has been described. In this study, we report an *in vivo* and *in vitro* interaction between PML and MDM2 which is independent of p53. Two separate regions of PML are recognized which can interact with MDM2. The C-terminal half of PML, encoded by residues 300–633, can interact with the central region of MDM2 which includes the MDM2 acidic domain. In addition, PML amino acids 1–200, which encode the RING-finger and most of the B box zinc binding motifs, can interact with the C-terminal, RING-finger containing region of MDM2. Interestingly, PML mutants in which sumoylation at lysine 160 was inhibited displayed an increased association with MDM2, suggesting that sumoylation at this site may be a determinant of PML-MDM2 binding. Coexpression with MDM2 caused a redistribution of PML from the nucleus to the cytoplasm, and this required the PML N terminus and the MDM2 RING-finger domain. These results suggest that interaction between the PML N terminus and MDM2 C terminus can promote PML nuclear exclusion. Wild-type MDM2 inhibited the ability of PML to stimulate the transcriptional activity of a GAL4-CBP fusion protein. This inhibition required the central, acidic region of MDM2, but did not require the MDM2 C terminus. Taken together, these studies demonstrate that MDM2 and PML can interact through at least two separate protein regions, and that these interactions can have specific effects on the activity and/or localization of PML.

Wild-type PML is a tumor suppressor and ubiquitously expressed nuclear phosphoprotein. The *PML* gene was originally identified as a result of a reciprocal translocation t(15:17) associated with acute promyelocytic leukemia (1–4). The t(15:17) translocation disrupts the *PML* gene on chromosome 15 and the retinoic acid receptor (RAR)[1] α (*RAR*α) gene on chromosome 17 and is reciprocal in nature, resulting in the generation of novel fusion proteins PML-RARα and RARα-PML (5). The most striking feature of wild-type PML is its localization to distinct nuclear foci that have been termed PML nuclear bodies (PML-NBs), Kremer bodies, ND10 or PODs (for PML oncogenic domains). These PML-NBs are multiprotein complexes that are 0.1–0.2 μm in diameter, and cells typically contain 10–30 PML-NBs/nucleus, although their number and size can vary during the cell cycle (6, 7). In acute promyelocytic leukemia cells, expression of PML-RARα causes disruption of PML-NBs and a redistribution of PML to a microspeckled nuclear localization pattern (8–10). PML-RARα can form heterodimers with wild-type PML (8, 10) as well as retinoid X receptor, another retinoic acid receptor family member (11). Current models suggest that sequestration of normal PML by PML-RARα inhibits the growth suppressive activity of PML, whereas sequestration of retinoid X receptor prevents the induction of differentiation (5). Inhibition of both of these pathways may be necessary for leukemogenesis.

The PML protein contains well characterized zinc binding domains in its N-terminal half, including a RING-finger adjacent to two cysteine/histidine-rich motifs known as B boxes. These domains, together with an α-helical coiled-coil domain, comprise a conserved motif known as RBCC (12). PML is covalently modified by SUMO-1, a small ubiquitin-like polypeptide also known as sentrin-1, UBL-1, or PIC-1 (13). Like ubiquitin, SUMO-1 is linked covalently to lysine residues on PML and other target proteins in an ATP-dependent manner (14). However, SUMO-1 modification seems to modulate the localization of its target proteins rather than induce their degradation. Three major sites for SUMO-1 modification were identified in PML: Lys-65 in the RING-finger, Lys-160 in the first B box, and Lys-490 in the nuclear localization signal (15, 16). Sumoylation of PML is essential for formation of PML-NBs and for its ability to recruit NB-associated proteins (17, 18). Sumoylation was also thought to be required for PML-dependent growth suppression. However, this latter hypothesis was challenged by a recent study in which a mutant PML deficient in sumoylation maintained its ability to inhibit growth when overexpressed (19).

The mechanisms by which PML functions as a tumor suppressor and inhibits growth have not been fully clarified. Mice with a targeted disruption of the PML locus (PML−/−) display

* This work was supported by NCI, National Institutes of Health Grant 1RO1CA80918–01 and American Cancer Society Grant RSG-01-042 (to C. G. M.). The costs of publication of this article were defrayed in part by the payment of page charges. This article must therefore be hereby marked "*advertisement*" in accordance with 18 U.S.C. Section 1734 solely to indicate this fact.

** To whom correspondence should be addressed: Dept. of Radiation Oncology, the University of Chicago, 5841 S. Maryland Ave., MC1105 Room G-06, Chicago, IL 60637. E-mail: cmaki@rover.uchicago.edu.

‡‡ Present address: Dept. of Cancer Biology, Cancer Research Center, University of Massachusetts Medical School, Worcester, MA 01605.

[1] The abbreviations used are: RAR, retinoic acid receptor; CBP, CREB-binding protein; CREB, cAMP enhancer-binding protein; GST, glutathione *S*-transferase; HA, hemagglutinin; NB, nuclear body; NLS, nuclear localization signal; wt, wild-type.

an increased incidence of carcinomas after treatment with tumor-promoting agents (20). Further, cells derived from PML−/− mice are resistant to apoptosis in response to various apoptotic stimuli (21). These results suggest that PML plays a central role in apoptosis signaling. A relationship between PML and p53 was suggested by the finding that p53 could interact directly with PML and was recruited by PML into PML-NBs (22). Subsequent studies have shown that PML corecruits both p53 and CBP/p300 to PML-NBs. CBP/p300 then promotes the acetylation of p53, which increases p53 DNA binding affinity and thus leads to an activation of p53-responsive genes (23, 24). Perhaps the most compelling evidence that links the PML and p53 growth-suppressive pathways comes from studies of oncogene-induced senescence. In these studies, p53 activity was measured in PML+/+ and PML−/− cells infected with retroviruses expressing an activated *ras* oncogene (Ras V12). Ras V12 expression in PML+/+ cells resulted in the activation of p53, recruitment of p53 into PML-NBs, and the induction of premature senescence. In contrast, p53 was neither activated nor recruited into PML-NBs in PML−/− cells, and the cells were resistant to *ras*-induced senescence (23, 24). These studies provide strong evidence that PML is required for the efficient activation of p53 in response to aberrant oncogene signaling.

p53 levels and activity are controlled in large part by MDM2, the product of a p53-inducible gene. MDM2 binds to the N terminus of p53 and inhibits the activity of p53 as a transcription factor (25, 26). Importantly, MDM2 binding also promotes the ubiquitination of p53 and its subsequent degradation by the proteasome, as well as the export of p53 from the nucleus to the cytoplasm (27–30). Insofar as PML and MDM2 have opposing effects on p53 activity, it is of interest to investigate the functional relationship between PML and MDM2. However, to date neither a physical nor functional interaction between PML and MDM2 has been described. The current report demonstrates an *in vivo* and *in vitro* interaction between PML and MDM2 which can occur independent of p53. Mapping studies indicate that PML and MDM2 can interact through at least two separate protein regions and that these interactions can affect both the localization and activity of PML.

EXPERIMENTAL PROCEDURES

Plasmid DNAs—FLAG-tagged PML expression DNA was obtained from Zhi-Min Yuan (Harvard School of Public Health). HA-tagged PML was generated from this clone by PCR. The 3′-primer for PCR was the SP6 primer (Promega), and the 5′-primer was 5′-GCGAATTCACCATGTACCCATACGATGTTCCAGATTACGCTGAGCCTGCACCCGCCCG-3′. The resulting PCR product was digested with *Eco*RI and *Xba*I restriction enzymes and cloned into the corresponding sites of pCDNA-3.1. All subsequent PML clones were generated by PCR using HA-PML wild-type as the template. N-terminal deletions of PML were generated using the SP6 primer as the 3′-primer, and the following 5′-primers: for HA-PML Δ100N, 5′-GCGAATTCACCATGTACCCATACGATGTTCCAGATTACGCTACACCCGCCCTGGATAACG-3′; for HA-PML Δ200N, 5′-GCGAATTCACCATGTACCCATACGATGTTCCAGATTACGCTAGCATCT ACTGCCGAGG-3′; for HA-PML Δ300N, 5′-GCGAATTCACCATGTACCCATACGATGTTCCAGATTACGCTGTGGACGCGCGGTACCAGC-3′; for HA-PML Δ400N, 5′-GCGAATTCACCATGTACCCATACGATGTTCCAGATTACGCTAAAGCCAGCCCAGAGGC-3′; PCR products were digested with *Eco*RI and *Xba*I restriction enzymes and cloned into the corresponding sites of pCDNA-3.1. Sumoylation site mutants of PML were generated using the QuikChange mutagenesis kit (Stratagene) and HA-PML wild-type as a template. For HA-PML (K65R), the following primer and its complement were used: 5′-GCGGAAGCCAGGTGCCCGAAGCTTCTGCCTTGTCTGC-3′. For HA-PML (K160R), the following primer and its complement were used in the PCR: 5′-CAGTGGTTCCTCAGGCTCGAGGCCCGGC-3′. For HA-PML (K490R), the following primer and its complement were used: 5′-GACCCAGTGCCCGCGGAAGGTCATCAGGATGGAGTCTGAGG-3′. C-terminal deletions of HA-PML (K160R) were generated using 5′-GCGAATTCACCATGTACCCATACGATGTTCCAGATTACGCTGAGCCTGCACCCGCC CG-3′ as the 5′-primer and the following 3′-primers: for HA-PML K160R (1–500), 5′-CCGTCTAGATCACCTTGCCTCCTTCCCCTCC-3′; for HA-PML K160R (1–400), 5′-CCGTCTAGATCACTTGGATACAGCTGCATC-3′; for HA-PML K160R (1–300), 5′-CCGTCTAGATCAAGCCTCCAGCAGCTCGCGC-3′; for HA-PML K160R (1–200), 5′-CCGTCTAGATCAGGTCAGCGTAGGGGTGCGG-3′. The resulting PCR products were digested with *Eco*RI and *Xba*I and cloned into the corresponding sites in pCDNA3.1. FLAG-tagged MDM2 DNAs were described (31, 32) and were obtained from Zhi-Min Yuan. FLAG-MDM2 ΔNT lacks 120 amino acids from the N terminus. DNAs encoding wild-type MDM2 and MDM2 Δ217–246 were obtained from Steve Grossman (Dana Farber Cancer Institute). FLAG-tagged MDM2 (2–202), (100–304) and (301–488) were generated by PCR using wild-type MDM2 DNA as a template. For MDM2 (301–488) the 5′-primer was 5′-CCGGGATCCCCAAAGAAGAAGAGGAAGGACTATTGGAAATGCACTTCATGC-3′, and the 3′-primer was 5′-CCGTCTAGATCAAGTTAGCACAATCATTTGAATTGG-3′. The resulting PCR products were digested with *Bam*HI and *Xba*I and cloned downstream and in-frame with the FLAG epitope in pCDNA3.1. MDM2 (301–488) contains the SV40 large-T antigen NLS encoded within the 5′-primer. For MDM2 (2–202) the 5′-primer was 5′-CCGGGATCCTGCAATACCAACATGTCTGTACC-3′, and the 3′-primer was 5′-CCGGAATTCTCATATTACACACAGAGCCAGGC-3′. For MDM2 (100–304) the 5′-primer was 5′-CCGGGATCCTATACCATGATCTACAGGAACTTGG-3′, and the 3′-primer was 5′-CCGGAATTCTCATTTCCAATAGTCAGCTAAGG-3′. The resulting PCR products were digested with *Bam*HI and *Eco*RI and cloned downstream and in-frame with the FLAG epitope in pCDNA3.1. MDM2 (6–339) was obtained from Arnold Levine.

Tissue Culture, Immunoblots, Immunoprecipitation—Human osteosarcoma cell lines Saos-2 cells (p53-null) and U2OS (p53 wild-type), and 35-2 cells (murine p53 and MDM2 double knockout) were grown in minimum essential medium supplemented with 10% fetal bovine serum, 100 μg/ml penicillin and streptomycin. Transfections in Saos-2 and U2OS cells were done using the calcium phosphate method in 35-mm dishes when the cells were ~80% confluent. 16–20 h after addition of the DNA precipitate, cells were washed twice with minimum essential medium minus serum and refed with minimum essential medium plus 10% fetal bovine serum. Cell extracts were prepared 8–10 h later. Transfections in 35-2 cells were done using FuGENE-6 (Roche Applied Science), according to the manufacturer's instructions. For immunoblot analysis and coimmunoprecipitations, cells were rinsed with phosphate-buffered saline and scraped into 500 μl of lysis buffer (50 mM Tris, pH 7.5, 5 mM EDTA, 150 mM NaCl, 0.5% Nonidet P-40, 1 mM phenylmethylsulfonyl fluoride, 2 μg/ml aprotinin, 5 μg/ml leupeptin). The scraped cells were lysed on ice for 30 min with occasional light vortexing, followed by a 15-min centrifugation to remove cellular debris. Protein extracts were then either immunoprecipitated or resolved by SDS-PAGE, and transferred to a PolyScreen polyvinylidene difluoride transfer membrane (PerkinElmer Life Sciences). Antibodies used for immunoblotting were the anti-HA monoclonal antibody (HA.11 from Babco), an anti-MDM2 monoclonal antibody (SMP-14 from Santa Cruz), or an anti-FLAG monoclonal antibody (M5 from Sigma). For immunoprecipitations, 300 μg of transfected cell extract was immunoprecipitated with 0.6 μg of the anti-HA polyclonal antibody Y-11 (from Santa Cruz) or 0.2 μg of anti-MDM2 (SMP-14). To detect sumoylated PML species, cells were rinsed with phosphate-buffered saline and scraped into 500 μl of radioimmunoprecipitation assay buffer (20 mM Tris, pH 7.5, 2 mM EDTA, 150 mM NaCl, 0.25% SDS, 1% Nonidet P-40, 1% deoxycholic acid), and then sonicated for 10 pulses (setting 5, 50% output) using a Branson-450 sonifier. Lysates were centrifuged for 15 min prior to analysis to remove cellular debris.

Immunofluorescence Staining—For immunofluorescence staining, cells were plated on glass coverslips and transfected, washed, and refed as described above. 24 h after transfection, cells were rinsed with phosphate-buffered saline plus 0.1 mM $CaCl_2$ and 1 mM $MgCl_2$ and fixed with 4% paraformaldehyde for 30 min at 4 °C. Paraformaldehyde was then replaced with 50 mM NH_4Cl for 5 min, and cells were permeabilized with 0.1% Triton X-100 plus 0.2% bovine serum albumin. PML staining was carried out using the anti-HA monoclonal antibody HA.11 (Babco) as the primary antibody and rhodamine red-conjugated anti-mouse antibody (Jackson Labs) as the secondary antibody. MDM2 staining was carried out using the anti-MDM2 polyclonal antibody N-20 (Santa Cruz) as the primary antibody, and either 7-amino-4-methylcoumarin-3-acetic acid-conjugated anti-rabbit antibody, or fluorescein isothiocyanate-conjugated anti-rabbit antibody (Jackson Labs) as the secondary antibody. Specimens were then examined under a fluorescent microscope.

GST Fusion Protein Production—GST-tagged PML wild-type DNA

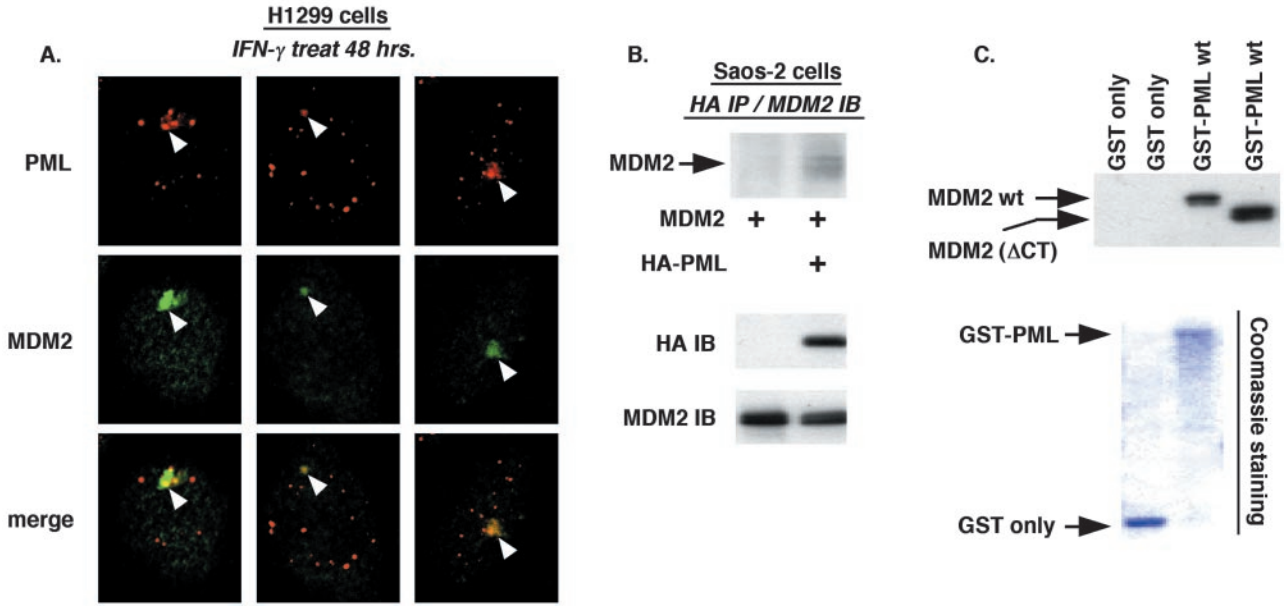

FIG. 1. **p53-independent interaction between MDM2 and PML.** *A*, H1299 cells (p53-null) were treated with 1,000 units/ml IFN-γ for 48 h and then examined by immunofluorescence staining with antibodies against PML and MDM2. Shown are three examples of the PML, MDM2, and merged images obtained by confocal microscopy. The *white arrow* in each case indicates the position in which there is colocalization of the endogenous PML and MDM2 proteins. *B*, Saos-2 cells (p53-null) were transfected with expression DNAs encoding MDM2 and HA-tagged PML, as indicated. Cell lysates were immunoprecipitated (*IP*) with an anti-HA polyclonal antibody and examined by immunoblotting (*IB*) with an antibody against MDM2. The *arrow* indicates MDM2 protein that was coimmunoprecipitated with HA-PML (*upper panels).* Steady-state levels of HA-PML and MDM2 were monitored by immunobloting of lysates without prior immunoprecipitation (*lower panels). C*, GST-PML wt or GST alone was generated in bacteria and tested for binding to partially purified MDM2 that was either wild-type or lacked either the C terminus (MDM2 ΔCT). Binding complexes were resolved by SDS-PAGE and examined by immunoblotting with an antibody against MDM2. The Coomassie-stained gel indicates the relative amount of each GST protein used in the binding reaction.

was generated by PCR using HA-PML wild-type as a template. The 3′-primer for PCR was 5′-GGCGCGGCCGCCTCACCAGGAGAACCCACTTTCATTG-3′, and the 5′-primer was 5′-CCGGGATCCGAGCCTGCACCCGCCCGATCTCCG-3′. The resulting PCR product was digested with *Bam*HI and *Not*I restriction enzymes and cloned into the corresponding sites of pGEX-4T-3. GST-tagged PML K160R DNA was generated by PCR using the same primers but HA-PML K160R as a template. DNAs encoding GST alone or GST-PML were used to transform BL-21 bacterial cells, and transformed cells were grown at 37 °C until reaching log phase. GST protein expression was induced by incubation in 0.2 mM isopropyl-1-thio-β-galactopyranoside for 3 h. To purify the GST proteins, cells were lysed by sonication in lysis buffer (10 mM Tris-HCl, pH 7.5, 1 mM EDTA, 0.1% Triton X-100, 150 mM NaCl), and the resulting lysate was incubated for 12 h at 4 °C with glutathione-Sepharose beads. The beads were pelleted by centrifugation and washed with lysis buffer. For MDM2 binding, the GST-tagged proteins bound to beads were incubated with MDM2 protein in 300 μl of lysis buffer for 5–6 h. Unbound MDM2 protein was removed by five washes (1 ml each) with lysis buffer. Bound proteins were eluted by boiling for 10 min in 1 × loading buffer, resolved by SDS-PAGE, and examined by immunoblot analysis with the anti-MDM2 antibody SMP-14.

Expression and Isolation of MDM2 from Insect Cells—DNA encoding FLAG-tagged MDM2 that was either wild-type, lacked amino acids 217–246 (MDM2 Δp300BD), or lacked the C-terminal RING domain between residues 443 and 491 (MDM2 ΔCT) was cloned into a baculovirus expression system and used for expression in insect cells. MDM2 protein was isolated by passing insect cell lysate over a column of Sepharose beads conjugated to an anti-FLAG antibody. Bound proteins were washed several times and eluted with a peptide encoding the FLAG epitope.

RESULTS

PML protein levels increase upon exposure of cells to interferons (IFNs) through direct transcriptional activation of the PML gene. To test for an *in vivo* interaction between PML and MDM2, H1299 cells (p53-null) were exposed to IFN-γ for 48 h to induce endogenous PML expression, and the cells were then examined by immunofluorescence staining and confocal microscopy with antibodies against MDM2 and PML. These studies revealed colocalization between the endogenous PML and MDM2 proteins in IFN-γ–treated H1299 cells (Fig. 1*A*). Because H1299 cells lack p53 expression, these results suggest that MDM2 and PML can form an endogenous complex, either directly or indirectly, in the absence of p53. We also attempted to coimmunoprecipitate PML and MDM2 from IFN-γ-treated H1299 cells (not shown). However, we have been unable to immunoprecipitate large amounts of endogenous PML using our normal cell lysis conditions because the PML protein is insoluble under these conditions. We can solubilize PML under relatively harsh lysis conditions (high detergent), but these conditions are denaturing and therefore destroy any putative PML-MDM2 interactions. To examine the PML-MDM2 interaction further, Saos-2 cells (p53-null) were transfected with DNAs encoding MDM2 and epitope-tagged (HA-tagged) PML. Cell lysates were then immunoprecipitated with an anti-HA antibody and examined by immunoblotting with an antibody against MDM2. As shown in Fig. 1*B*, MDM2 coimmunoprecipitated with HA-PML in Saos-2 cells, again demonstrating that MDM2 and PML can interact in the absence of p53. To test the possibility that MDM2 and PML may interact directly, wild-type PML protein fused to GST was generated in bacteria, purified on glutathione-agarose beads, and mixed with partially purified, recombinant MDM2 protein produced in insect cells. Association between PML and MDM2 was then assessed in GST pull-down assays. As shown in Fig. 1*C*, wild-type (wt) MDM2 formed a complex with GST-PML wt, whereas no complex was observed between MDM2 and the GST protein alone. These results indicate that MDM2 and PML can interact with each other and suggest that this may be a direct interaction. An MDM2 protein lacking the C-terminal amino acids 443–491 (MDM2 ΔCT) also formed a complex with GST-PML wt but not with the GST protein control, indicating that this *in vitro* binding between PML and MDM2 does not require the MDM2 C terminus.

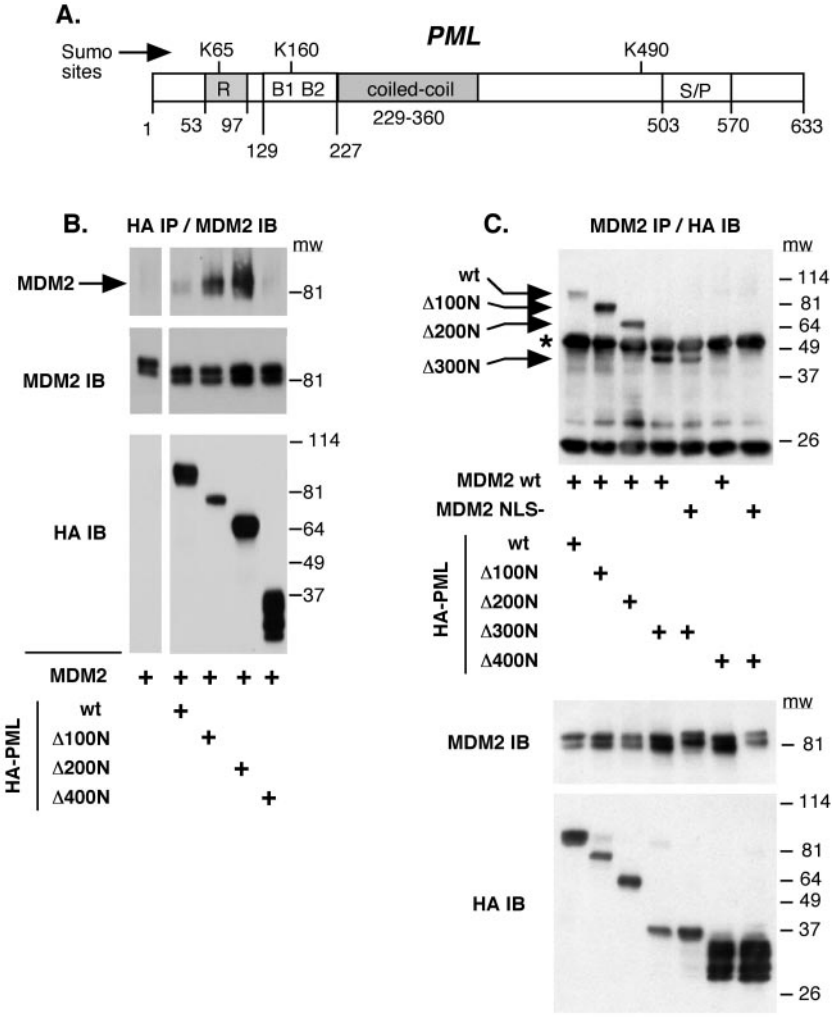

FIG. 2. **Binding of PML deletion mutants to MDM2.** *A*, schematic of the PML protein showing the positions of the RING-finger domain (*R*), the two B box zinc binding domains (*B1*, *B2*), the predicted α-helical coiled-coil, and the three sites of sumoylation. *B*, U2OS cells were transfected with DNAs encoding wild-type MDM2 and either wild-type PML or the indicated deletion mutant of PML. PML protein was precipitated with an anti-HA antibody, and the immunoprecipitates (*IP*) were examined with an antibody against MDM2 (*top panel*). Steady-state levels of HA-PML and MDM2 were monitored by immunobloting (*IB*) of lysates without prior immunoprecipitation (*middle* and *lower panels*). The molecular mass (*mw*) in kDa of protein standard is indicated next to each blot. *C*, U2OS cells were transfected with DNAs encoding either wild-type MDM2 or an MDM2 mutant that localizes in the cytoplasm (MDM2 NLS-), and the indicated form of HA-PML. MDM2 protein was precipitated with an anti-MDM2 antibody, and the immunoprecipitates were examined with an antibody against HA (*top panel*). Steady-state levels of HA-PML and MDM2 were monitored by immunobloting of lysates without prior immunoprecipitation (*middle* and *lower panels*).

We next wished to identify the regions of PML and MDM2 required for their interaction. PML contains several well characterized protein domains, including a RING-finger, two B boxes, and an α-helical coiled-coil (Fig. 2*A*) (for review, see Ref. 12). To map the regions of PML required for MDM2 binding, N-terminal deletion mutants of HA-PML were expressed with MDM2 in transiently transfected cells. Cell lysates were then immunoprecipitated with an anti-HA antibody and examined by immunoblotting with an antibody against MDM2. As shown in Fig. 2*B*, MDM2 coimmunoprecipitated with HA-tagged wild-type PML, consistent with the results of Fig. 1. Interestingly, deletion mutants of PML lacking 100 or 200 amino acids from the N terminus displayed a much stronger interaction with MDM2 compared with wild-type PML, whereas a PML deletion mutant lacking 400 amino acids from the N terminus was unable to bind MDM2. Similar binding results were obtained in the reciprocal coimmunoprecipitation, which involved first immunoprecipitating with an anti-MDM2 antibody, followed by immunoblotting with an anti-HA antibody (Fig. 2*C*). In these studies, wild-type PML again displayed relatively weak binding to MDM2, whereas mutants lacking 100, 200, or 300 amino acids from the PML N terminus displayed stronger association with MDM2, and a mutant lacking 400 amino acids from the N terminus failed to bind MDM2. These results indicate that the C-terminal region of PML between residues 300 and 633 can form a complex with MDM2 and suggest that sequences within the N terminus of PML may be inhibitory to this PML-MDM2 complex formation.

Wild-type PML is post-translationally modified by the covalent attachment of SUMO, a small ubiquitin-like molecule, at three separate lysine residues in the PML sequence (Lys-65, Lys-160, and Lys-490; Fig. 2*A*) (13, 15, 16). Sumoylation is mediated by the sumo-conjugating enzyme Ubc9 and requires interaction between Ubc9 and the RING-finger domain within the first 100 amino acids of PML (16). The finding that PML mutants lacking the first 100 amino acids displayed an increased association with MDM2 suggested that sumoylation of PML may be inhibitory to PML-MDM2 binding. To investigate this possibility, PML mutants were generated in which each sumo site lysine was converted to arginine either singly or in combination, and association between these mutants and MDM2 was monitored by coimmunoprecipitation. As shown in Fig. 3*A*, MDM2 coimmunoprecipitated with wild-type PML to a relatively small extent in cells transiently expressing both proteins. MDM2 also coimmunoprecipitated with PML K65R and PML K490R to a comparable extent. In contrast, the PML K160R and PML 3KR mutants displayed a much stronger association with MDM2 compared with either wild-type PML or the other sumo site mutants. These findings suggested that PML sumoylation at lysine 160 may be an important regulator of MDM2 binding. In light of these results, we wished to confirm the sumoylation status of PML that coimmunoprecipitates with MDM2. Sumoylated PML is largely insoluble under gentle conditions of cell lysis. Therefore, to observe sumoylated PML, transfected cells were lysed in buffer containing a relatively high detergent concentration (radioimmunoprecipitation

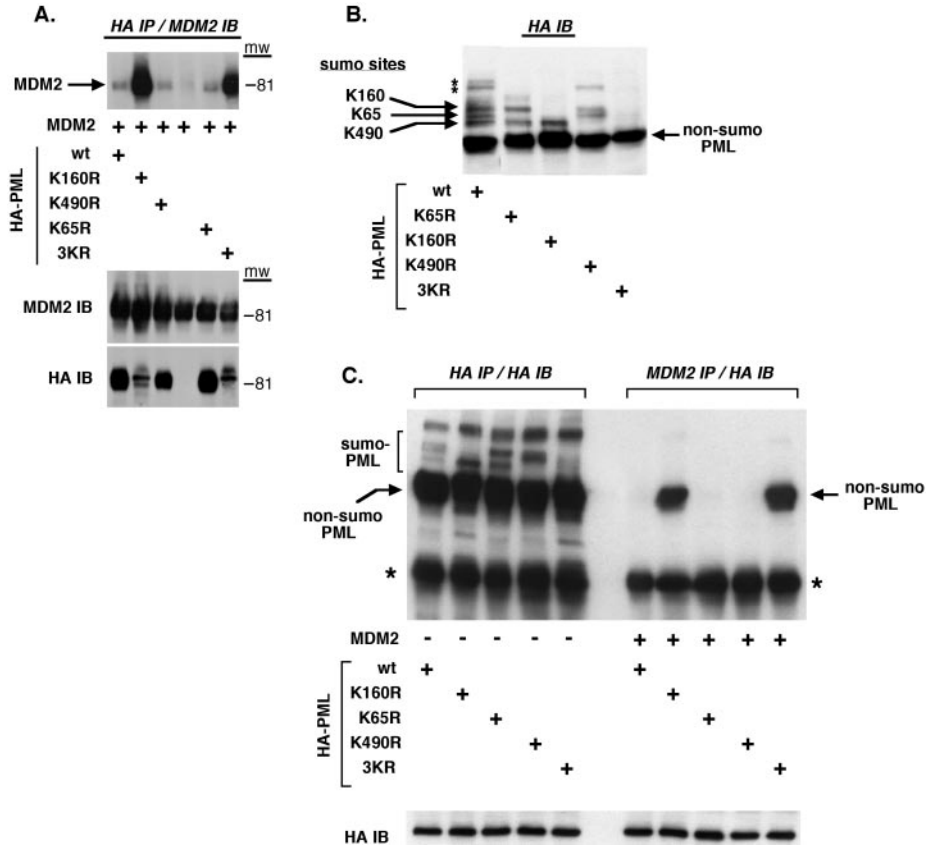

FIG. 3. **Binding of MDM2 to PML sumoylation site mutants.** *A*, U2OS cells were transfected with DNAs encoding wild-type MDM2 and either wild-type PML or the indicated sumoylation site mutants of PML. PML protein was precipitated with an anti-HA antibody (*IP*), and the immunoprecipitates were examined with an antibody against MDM2 (*top panel*). Steady-state levels of HA-PML and MDM2 were monitored by immunobloting (*IB*) of lysates without prior immunoprecipitation (*middle* and *lower panels*). *B*, cells were transfected with DNAs encoding the indicated forms of HA-PML. The cells were then lysed in radioimmunoprecipitation buffer with sonication, as described under "Experimental Procedures," and examined by immunoblotting with an anti-HA antibody. The position of nonsumoylated PML, as well as PML sumoylated at lysine 65, 160, and 490, are indicated. The *asterisks* (*) indicate higher molecular mass bands that are most likely forms of HA-PML which are sumoylated at multiple sites. *C*, cells were transfected with DNAs encoding MDM2 and the indicated form of HA-PML. Cell lysates were immunoprecipitated with either an anti-HA antibody or an anti-MDM2 antibody, and the immunoprecipitates were examined with an anti-HA antibody (*upper panels*). The nonsumoylated and sumoylated forms of PML are indicated. The *asterisk* indicates the position of the antibody heavy chain used in the immunoprecipitation. Steady-state levels of HA-PML were monitored by immunobloting of lysates without prior immunoprecipitation (*lower panels*).

buffer) and subsequently examined by immunoblotting with an anti-HA antibody. These studies revealed a series of high molecular mass PML species that migrated above wild-type HA-PML and each of the single sumo site mutants (Fig. 3*B*). Comparing the pattern of these species allowed us to identify each as PML that is sumoylated at Lys-65, Lys-160, or Lys-490. In contrast, these high molecular mass bands were not detected with expression of the PML 3KR mutant. To characterize the sumoylation state of PML bound to MDM2, wild-type PML and each of the sumo site mutants were expressed either alone or with MDM2. Transfected cells were then immunoprecipitated with either an anti-HA or anti-MDM2 antibody and examined by immunoblotting with an anti-HA antibody (Fig. 3*C*). In these studies the K160R and 3KR PML mutants again showed a much stronger association with MDM2 than the other forms of PML, and only the nonsumoylated PML species could be coimmunoprecipitated with MDM2. Taken together, these results indicate that nonsumoylated PML is the primary form of PML that coimmunoprecipitates with MDM2 and suggest that sumoylation at lysine 160 may be inhibitory to PML-MDM2 binding.

The strong interaction between HA-PML K160R and MDM2 allowed us to use this mutant in mapping other PML regions that may potentially interact with MDM2. To this end, C-terminal deletion mutants of HA-PML K160R were tested for MDM2 binding by coimmunoprecipitation. Because the nuclear localization signal (NLS) of PML is located in the C terminus between residues 487 and 493, C-terminal deletion mutants that lack the NLS may localize in the cytoplasm rather than the nucleus. Therefore, a cytoplasmic, NLS mutant of MDM2 was included in these studies to ensure colocalization of the transfected proteins. As shown in Fig. 4, full-length HA-PML (K160R) formed a strong complex with MDM2 in cotransfected cells. Similarly, C-terminal deletion mutants of HA-PML (K160R) also formed a strong complex with either wild-type MDM2 or the MDM2 NLS mutant, including a deletion mutant encoding only residues 1–200. In these studies, the C-terminal deletion mutants of HA-PML (K160R) displayed varying degrees of binding to either wild-type MDM2 or the MDM2 NLS mutant. Forms of PML (K160R) that are 1–633 and 1–500 contain the NLS and localize to the nucleus of transfected cells (not shown). These forms of HA-PML (K160R) bind most strongly to the nuclear localized wild-type MDM2 protein. In contrast, HA-PML (K160R) 1–400 lacks the NLS and localizes to the cytoplasm, unable to enter the nucleus without being actively imported. Not surprisingly, HA-PML (K160R) 1–400 associates strongly with the cytoplasmic MDM2 NLS mutant and only weakly with wild-type MDM2. The smaller HA-PML (K160R) mutants (1–300 and 1–200) also lack the NLS but are small enough to diffuse freely in and out of the nucleus, at least

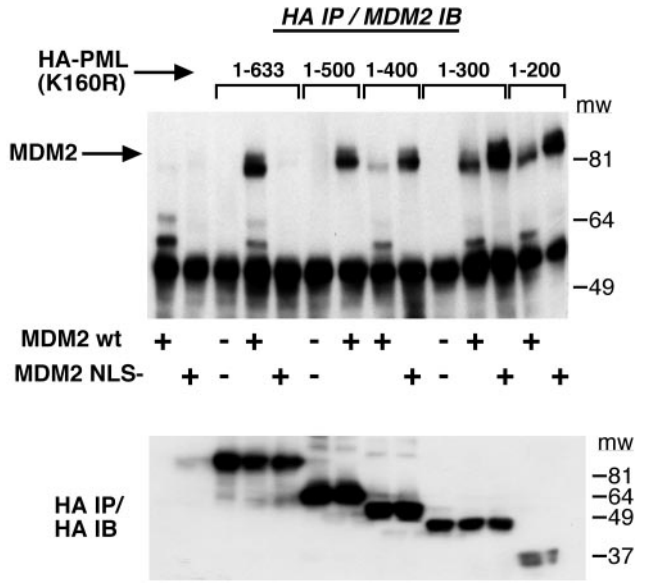

FIG. 4. **Recognition of an MDM2 binding region within the PML N terminus.** Cells were transfected with DNAs encoding wild-type MDM2 or MDM2 (NLS-) either alone or cotransfected with the indicated deletion mutants of HA-PML (K160R). Transfected cell lysates were immunoprecipitated (*IP*) with an anti-HA antibody and examined by immunoblotting (*IB*) with an antibody against MDM2 (*upper panel*). The *asterisk* indicates the position of the antibody heavy chain used in the immunoprecipitation. Reprobing of the blot with an anti-HA antibody shows the expression level of the transfected PML proteins (*lower panel*).

to some extent. These forms of HA-PML (K160R) display a diffuse localization pattern throughout the cell (not shown) and can bind both nuclear wild-type MDM2 and the cytoplasmic MDM2 NLS mutant. These results demonstrate that residues 1–200 in PML-K160R encode a separate MDM2 binding region. It should be noted that PML residues 1–200 (wild-type) displayed little to no binding to MDM2 when tested in a coimmunoprecipitation study similar to that shown in Fig. 4 (data not shown), consistent with the hypothesis that the K160R mutation uncovers an MDM2 binding site in this region of PML which would otherwise not be evident.

Our results indicate the presence of multiple MDM2 binding domains in PML, one located in the C terminus between residues 300 and 633, and a second that is revealed by the K160R mutation and is located between residues 1 and 200. We wished to define the regions of MDM2 required for interaction with either of these two regions of PML. To this end, MDM2 deletion mutants lacking various portions of the N terminus, C terminus, or central region were tested for their ability to coimmunoprecipitate with a form of PML which contained both binding domains (PML 1–633 (K160R)), or with PML mutants that expressed either MDM2 binding region alone. The results of these studies are summarized in Fig. 5. PML 1–633 (K160R), which contains both MDM2 binding regions, formed a strong complex with all of the MDM2 deletion mutants tested. This suggests the presence of multiple PML binding regions in MDM2, the deletion of any one of which may have little effect on PML binding. PML Δ200N also formed a complex with all of the tested MDM2 mutants, although lesser binding was observed between this form of PML and an MDM2 mutant that lacked the acidic domain between residues 222 and 272. This suggests that MDM2 residues between 222 and 272 may be required for strong interaction between MDM2 and the C-terminal half of PML. PML 1–200 (K160R) formed a complex with each MDM2 mutant except one that lacked the C terminus (MDM2 6–339), suggesting that MDM2 residues between 340 and 491 are required for interaction with HA-PML 1–200 (K160R). To map the PML interacting regions further, MDM2 mutants that expressed only the N terminus, C terminus, or central regions were tested in coimmunoprecipitation studies for binding to either PML 1–200 (K160R) or PML Δ200N (Fig. 5). In these studies, PML 1–200 (K160R) formed a strong complex with the C terminus of MDM2 (residues 300–488), but not with the MDM2 N terminus (residues 2–202) or central region (residues 100–304), demonstrating that the MDM2 C terminus can form a specific complex with residues 1–200 in PML-K160R. In contrast, PML Δ200N could be coimmunoprecipitated with MDM2 mutants encoding the central region between residues 100 and 304, but not with MDM2 mutants that encoded only the N (residues 2–202) or C (residues 300–488) terminus. These results are consistent with the observation that PML Δ200N displayed weak binding to an MDM2 mutant that lacked the central acidic domain (residues 222–272). In summary, these studies indicate that the C terminus of MDM2 can form a complex with PML residues 1–200 in the K160R mutant, whereas the MDM2 central region, which includes the acidic domain between residues 222 and 272, can interact with the C-terminal half of PML (Fig. 5).

Having identified multiple interactions between PML and MDM2, we next wished to determine the consequence of these interactions on the localization and/or activity of PML. The most striking feature of PML is its localization into multiprotein, nuclear foci structures, PML-NBs (33). Although the functions of PML are not fully understood, their proper localization and ability to recruit and interact with other NB components are considered essential for PML to act as a tumor suppressor (33, 34). To assess the effect of MDM2 on PML localization, cells were transfected with DNAs encoding HA-tagged PML either alone or cotransfected with various forms of MDM2. Localization of the transfected PML and MDM2 proteins was then monitored by immunofluorescence staining. As illustrated in Fig. 6*A*, HA-PML (wild-type) and MDM2 localized almost exclusively to the nucleus when expressed alone. In contrast, coexpression with wild-type MDM2 caused a marked redistribution of PML to the cytoplasm, whereas the MDM2 protein remained nuclear (Fig. 6*B*). These results indicated that nuclear MDM2 could trigger a redistribution of PML from the nucleus to the cytoplasm. We scored the extent to which PML was localized to the cytoplasm when expressed alone or with MDM2, and the results are graphed in Fig. 7. We next wished to investigate the region of MDM2 which may be required to promote this nuclear exclusion of PML. As shown in Figs. 6 and 7, MDM2 deletion mutants lacking either the central acidic domain (Δ222–272) or the N-terminal p53 binding domain (Δ120N) could efficiently promote the nuclear exclusion of PML, indicating that neither the central domain nor p53 binding domain is required for this effect. Similar results were obtained in Saos-2 cells (p53-null; data not shown), further demonstrating that MDM2 can promote PML nuclear exclusion in the absence of p53. An MDM2 mutant lacking the C terminus (MDM2 6–339) failed to promote PML nuclear exclusion (Figs. 6 and 7), suggesting that PML binding to the MDM2 C terminus may be required for this effect. Consistent with this hypothesis, an N-terminal deletion mutant of PML (HA-PML (Δ200N)) was completely resistant to MDM2-mediated nuclear exclusion. Given that the MDM2 C terminus can interact with the PML N terminus, these results suggest that binding between the N terminus of PML and the C terminus of MDM2 is required to promote the nuclear exclusion of PML.

One NB-associated protein with which PML interacts is the transcriptional coactivator CBP. PML binding has been reported to stimulate the ability of a GAL4-CBP fusion protein to

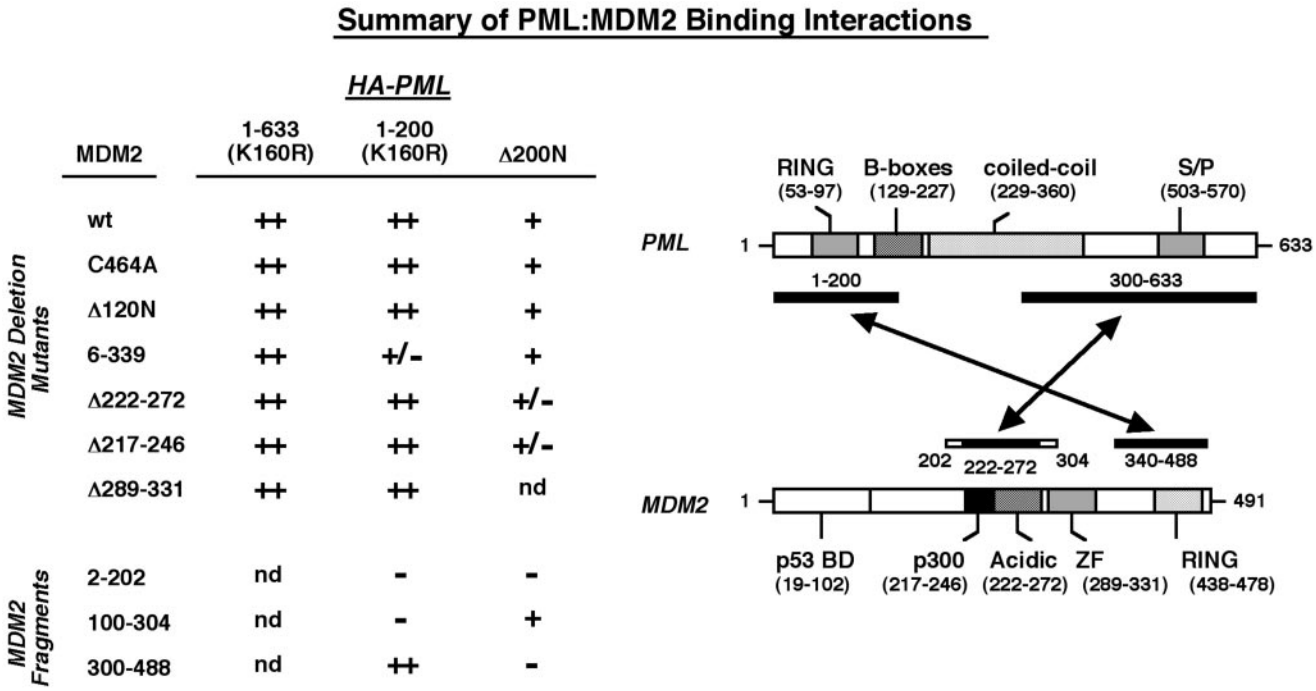

FIG. 5. **Summary of PML-MDM2 binding reactions.** The indicated forms of MDM2 and PML were coexpressed in transfected cells and examined for binding by coimmunoprecipitation. + indicates that binding was observed, − indicates that no binding was observed, and +/− indicates that weak binding was observed. *nd* indicates a combination of mutant MDM2 and PML that was not tested for binding (not done). The *schematic* on the *right* illustrates the proposed interactions between MDM2 and PML. The *solid bars* indicate the regions of each protein which are proposed to interact. PML amino acids 1–200 in the K160R mutant can interact with the C terminus of MDM2, probably between residues 340 and 488. PML amino acids 300–633 contain a second MDM2 binding region (see Fig. 2). HA-PML Δ200N could coimmunoprecipitate with the central region of MDM2 (amino acids 100–304) but not with the MDM2 N terminus (amino acids 2–202), suggesting that MDM2 residues between 202 and 304 are required. The MDM2 acidic domain (residues 222–272) also appears to be required for strong interaction with the C-terminal region of PML because HA-PML Δ200N displayed weaker interaction with an MDM2 mutant that lacks this region (MDM2 Δ222–272).

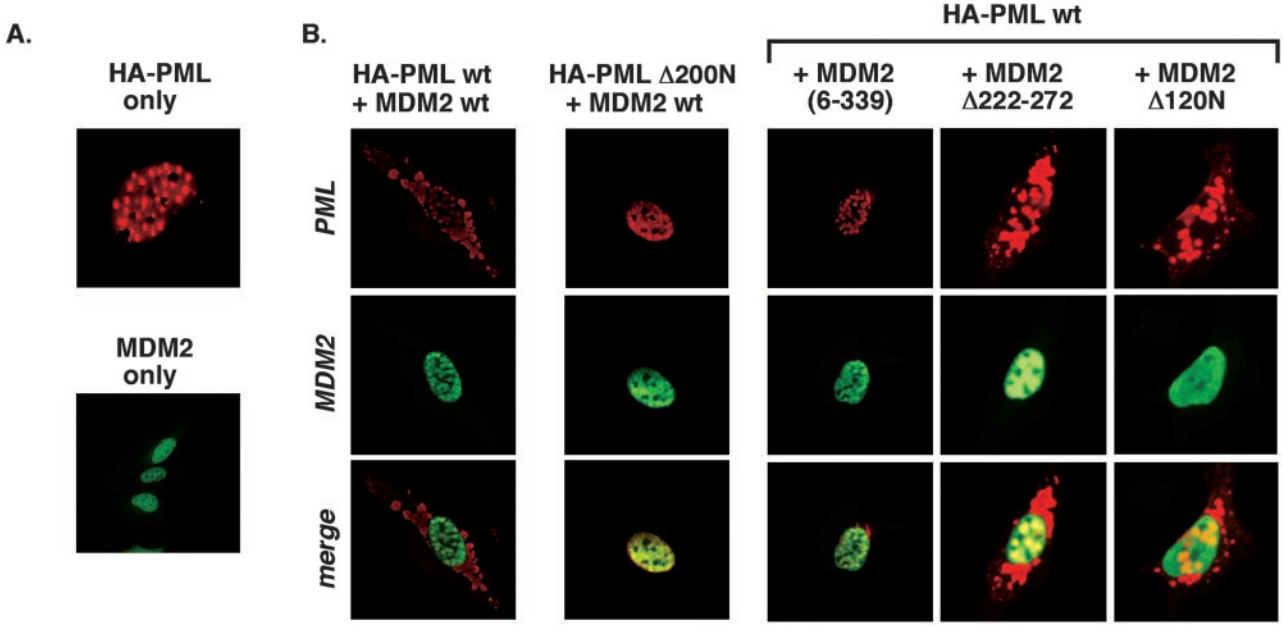

FIG. 6. **MDM2 promotes nuclear exclusion of PML in transiently transfected cells.** U2OS cells were transfected with DNAs encoding HA-PML (wild-type) or HA-PML (Δ200N), either alone or with the indicated forms of MDM2, and examined by immunofluorescence staining with anti-HA and anti-MDM2 antibodies. *A*, representative immunofluorescence staining patterns are shown for HA-PML (wild-type) and MDM2 (wild-type) when expressed alone. *B*, representative immunofluorescence staining patterns are shown for each transfection condition.

activate transcription from a gene promoter containing GAL4 DNA binding sites (35). We wished to test whether MDM2 could block the ability of PML to activate CBP. As shown in Fig. 8, HA-PML activated GAL4-CBP-dependent transcription, consistent with previous studies (35). Coexpression of wild-type MDM2 decreased the ability of PML to activate GAL4-CBP, although having relatively little effect on the activity of GAL4-CBP alone. These results indicate that wild-type MDM2 can inhibit the ability of PML to activate the GAL4-CBP fusion protein. To address the region of MDM2 required for this effect, we tested various MDM2 deletion mutants for their ability to inhibit PML in this assay. As shown in Fig. 8, the C-terminal

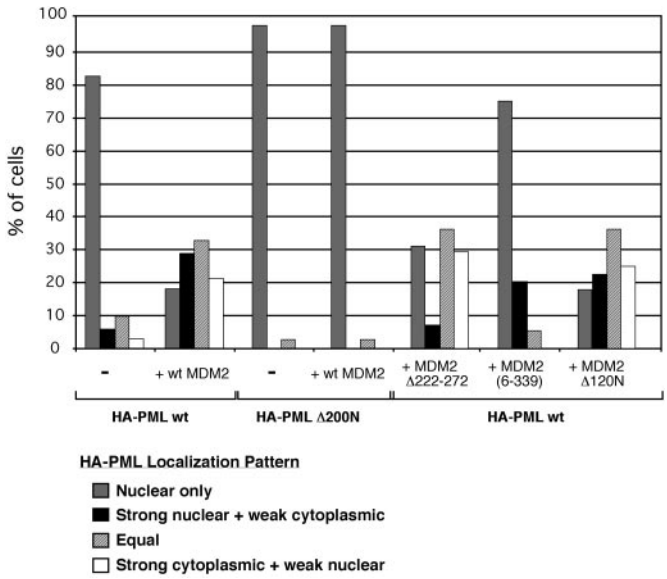

FIG. 7. **Quantification of MDM2-mediated nuclear exclusion of PML.** Cells were transfected with the indicated combinations of HA-PML and MDM2 and examined by immunofluorescence staining. The localization pattern for HA-PML in each case was scored for 150 cells in three separate experiments. The graph illustrates the average results from three separate experiments and shows the percentage of cells with the indicated HA-PML staining patterns. MDM2 exhibited complete nuclear staining in >90% of transfected cells when expressed alone or when coexpressed with HA-PML. Cells in which MDM2 did not exhibit complete nuclear staining were excluded from the analysis.

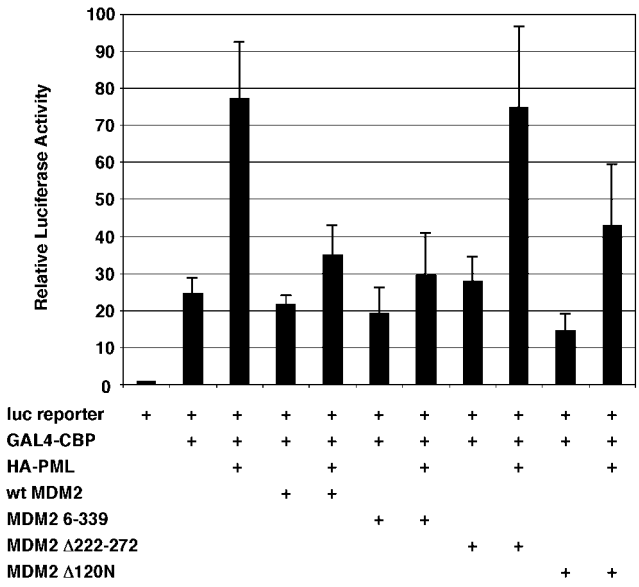

FIG. 8. **MDM2 inhibits PML-dependent activation of GAL4-CBP.** *A*, 35-2 cells (p53 and MDM2 double knockout) were transfected with a GAL4-responsive luciferase promoter and DNAs encoding GAL4-CBP (125 ng), HA-PML (200 ng), and the indicated forms of MDM2 (500 ng). Relative luciferase activity mediated by the GAL4-CBP fusion protein was measured. The graph shows the average results from three to seven independent experiments (±S.E.).

deletion mutant MDM2 (6–339) efficiently inhibited the ability of PML to activate the GAL4-CBP fusion protein. These results indicate that binding between the MDM2 C terminus and PML is not required to inhibit PML in this assay. Given that MDM2 (6–339) is unable to promote PML nuclear exclusion, these results also indicate that nuclear exclusion is not required for the MDM2-mediated inhibition of PML. An MDM2 mutant that lacks the N terminus (MDM2 Δ120N) was also able to inhibit the ability of PML to activate the GAL4-CBP fusion protein. In contrast, an MDM2 deletion mutant lacking residues 222–272 had little to no effect on the ability of PML to activate the GAL4-CBP fusion protein. These results indicate that the ability of MDM2 to inhibit PML in this assay requires the central, acidic region of MDM2 and therefore likely involves binding between the central region of MDM2 and PML.

DISCUSSION

The tumor suppressor protein PML has received considerable attention recently due, at least in part, to its involvement in apoptosis signaling and its direct interaction with p53. PML binding recruits p53 to PML-NBs, multiprotein complexes that localize to discreet foci within the nucleus. The effect of p53-PML binding is to increase p53 activity as a transcription factor (22). Current models suggest that recruitment to PML-NBs brings p53 in close proximity with CBP/p300 (36). Acetylation of p53 by CBP/p300 then increases p53 DNA binding affinity, leading to an activation of p53-responsive genes. This activation of p53 most likely contributes to the tumor suppressor function of PML. In addition to p53, PML can interact with a variety of other proteins and colocalize with them in PML-NBs. Included among these are proteins involved in recombination (BLM, RAD51, RAD52), transcriptional activation and repression (CBP, Daxx, Sp100), protein degradation (HAUSP, PA28), and the regulation of cell growth (pRB) (for review, see Refs. 37 and 38). However, in most cases the physiologic relevance of these interactions and their effect on cell proliferation have not been clarified fully.

The current report identifies MDM2 as a novel PML-interacting protein. Confocal microscopy revealed colocalization between the endogenous PML and MDM2 proteins in IFN-γ–treated H1299 cells (p53-null), suggesting that they can complex one another in cells. Further, MDM2 immunoprecipitated with PML in cells transiently expressing both proteins, and recombinant MDM2 produced in insect cells formed a strong complex with a bacterially expressed GST-PML fusion protein. These results indicate that MDM2 and PML can interact with each other in a manner independent of p53 and suggest that this may be a direct interaction. Mapping studies revealed at least two separate regions of MDM2 and PML involved in their interaction. First, the central region of MDM2, which includes the MDM2 acidic domain, could form a complex with the C-terminal portion (residues 200–633) of PML. The C terminus of PML is of particular interest when considering interactions between PML and other proteins. At least seven different PML isoforms have been described, all of which vary in their C termini and are generated by alternative splicing (12). It will be of interest in the future to determine whether interaction with the central region of MDM2 is an activity shared by all PML isoforms or occurs in an isoform-specific manner. The C terminus of MDM2 (residues 300–488) could also form a complex with residues 1–200 in the PML K160R mutant. The N terminus of PML and the C terminus of MDM2 both contain a RING-finger domain within their sequences, and we considered that the interaction between these two regions might be mediated through their respective RING-fingers. However, preliminary results from our laboratory suggest that the PML RING-finger is not required for residues 1–200 to interact with MDM2 (not shown), suggesting that this interaction with MDM2 is not through their corresponding RINGs. Interestingly, the extent to which MDM2 could bind PML in coimmunoprecipitation experiments was increased markedly when sumoylation of PML at lysine 160 was inhibited, either through deletion of PML protein regions required for Lys-160 sumoylation or through mutation of the Lys-160 site. This finding raises the possibility that PML sumoylation at Lys-160 may in some way be inhibitory to PML-MDM2

binding. Lys-160 is located within the N-terminal region of PML which can interact with the MDM2 C terminus. One possibility, therefore, is that sumoylation at this site blocks access of this region of PML to MDM2. However, it should be noted that sumoylation at Lys-160 is required for the proper localization of PML into PML-NBs (39, 40). A second possibility, therefore, is that sumoylation at Lys-160 may indirectly affect PML-MDM2 coimmunoprecipitation by directing PML into PML-NBs.

PML is the major component of multiprotein, nuclear foci structures, PML-NBs (33, 34). PML appears to be absolutely required for NB formation, as other NB-associated proteins fail to localize in NBs when PML is not present (39, 40). However, the biochemical and molecular functions of PML-NBs are still unknown. Most current models propose that PML-NBs are nuclear scaffolds that serve as either temporary storage sites for catalytically active proteins or as catalytic surfaces where specific biochemistries can occur (34). In either case, proper localization of PML, as well as its ability bind and recruit other NB-associated proteins, is considered essential for PMLs normal function. We observe that transient overexpression of MDM2 disrupts PML-NBs and promotes a redistribution of PML to the cytoplasm. Given the importance of proper localization in PML function, it is possible that MDM2 may inhibit one or more activities associated with PML through this disruption of its normal localization. The C terminus of MDM2 (residues 340–488) is necessary to alter PML localization, and the N terminus of PML is also required for PML to be redistributed to the cytoplasm by MDM2 (Figs. 6 and 7). Given the interaction between the PML N terminus and MDM2 C terminus, these results suggest that binding between these two regions is responsible for the cytoplasmic redistribution of PML. It is interesting to note that the disruption of PML-NBs and cytoplasmic redistribution of PML observed here with MDM2 overexpression is strikingly similar to the effect of certain viral proteins on PML. During a variety of viral infections, including those of the herpes, adeno, and retro families, PML-NBs become disrupted, and, in some cases, PML is relocalized to the cytoplasm (41–45). This disruption of PML-NBs has been linked in some cases to host cell shut-off, inhibition of apoptosis, and establishment of a chronic viral infection (45). In contrast, PML and other proteins associated with PML-NBs are induced after exposure to antiviral IFNs, and the number of PML-NBs increases (46). Based on these findings it has been proposed that PML-NBs may represent preferential targets for viral infections and that PML could play a role in the mechanism of the antiviral action of IFNs. Viral proteins that disrupt PML-NBs and/or cause a relocalization of PML to the cytoplasm include the herpes simplex virus type-1 ICP0 protein, the adenovirus E4-ORF-3 protein, the human cytomegalovirus IE1 protein, the lymphocytic choriomeningitis virus Z protein, and the rabies virus P protein (45; for review, see Ref. 46). Like MDM2, the herpes simplex virus type-1 ICP0 and lymphocytic choriomeningitis virus Z proteins both contain a RING-finger domain. Further, lymphocytic choriomeningitis virus Z and rabies P protein cause a cytoplasmic relocalization of PML, and herpes simplex virus type-1 ICP0 promotes the proteasome-dependent degradation of PML. It remains to be seen whether the relocalization of PML observed here with MDM2 expression occurs through a similar or distinct mechanism as in cells expressing these viral proteins.

CBP is a transcriptional activator with histone acetyltransferase activity and is a component of PML-NBs (47). PML forms a direct complex with CBP, and this complex formation stimulates the ability of a GAL4-CBP fusion protein to activate gene transcription (35). In the current report, wild-type MDM2 inhibited the ability of PML to activate GAL4-CBP-mediated transcription. This inhibition required the central, acidic region of MDM2, suggesting that binding between the central region of MDM2 and PML is required to inhibit PML in this assay. An MDM2 mutant that lacked the C terminus, and was therefore unable to redistribute PML to the cytoplasm, also inhibited the ability of PML to activate CBP. These results indicate that the MDM2-mediated nuclear exclusion of PML is not required for MDM2 to inhibit PML, at least in this assay system. Functional interactions among PML, MDM2, and CBP are of particular interest with regard to the PML-mediated activation of p53. Current models suggest that PML corecruits p53 and CBP to PML-NBs, bringing them into close proximity (for review, see Ref. 36). CBP can then acetylate p53, resulting in an increased p53 DNA binding activity, thus leading to an activation of p53-responsive genes. This activation of p53 most likely contributes to the tumor suppressor function of PML. Conceivably, MDM2 could inhibit this activation of p53 by either disrupting PML-NBs or blocking the ability of PML to activate CBP. Such a mechanism could contribute to the MDM2-mediated inhibition of p53.

REFERENCES

1. de The, H., Lavau, C., Marchio, A., Chomienne, C., Degos, L., and Dejean, A. (1991) *Cell* **66,** 675–684
2. Goddard, A. D., Borrow, J., Freemont, P. S., and Solomon, E. (1991) *Science* **254,** 1371–1374
3. Kakizuka, A., Miller, W. H., Jr., Umesono, K., Warrell, R. P., Jr., Frankel, S. R., Murty, V. V., Dmitrovsky, E., and Evans, R. M. (1991) *Cell* **66,** 663–674
4. Pandolfi, P. P., Grignani, F., Alcalay, M., Mencarelli, A., Biondi, A., LoCoco, F., Grignani, F., and Pelicci, P. G. (1991) *Oncogene* **6,** 1285–1292
5. Pandolfi, P. P. (2001) *Hum. Mol. Genet.* **10,** 769–775
6. Koken, M. H., Linares-Cruz, G., Quignon, F., Viron, A., Chelbi-Alix, M. K., Sobczak-Thepot, J., Juhlin, L., Degos, L., Calvo, F., and de The, H. (1995) *Oncogene* **10,** 1315–1324
7. Everett, R. D., Lomonte, P., Sternsdorf, T., van Driel, R., and Orr, A. (1999) *J. Cell Sci.* **112,** 4581–4588
8. Dyck, J. A., Maul, G. G., Miller, W. H., Jr., Chen, J. D., Kakizuka, A., and Evans, R. M. (1994) *Cell* **76,** 333–343
9. Koken, M. H., Puvion-Dutilleul, F., Guillemin, M. C., Viron, A., Linares-Cruz, G., Stuurman, N., de Jong, L., Szostecki, C., Calvo, F., and Chomienne, C. (1994) *EMBO J.* **13,** 1073–1083
10. Weis, K., Rambaud, S., Lavau, C., Jansen, J., Carvalho, T., Carmo-Fonseca, M., Lamond, A., and Dejean, A. (1994) *Cell* **76,** 345–356
11. Perez, A., Kastner, P., Sethi, S., Lutz, Y., Reibel, C., and Chambon, P. (1993) *EMBO J.* **8,** 3171–3182
12. Jensen, K., Shiels, C., and Freemont, P. S. (2001) *Oncogene* **49,** 7223–7233
13. Boddy, M. N., Howe, K., Etkin, L. D., Solomon, E., and Freemont, P. S. (1996) *Oncogene* **13,** 971–982
14. Seeler, J. S., and Dejean, A. (2001) *Oncogene* **20,** 7243–7249
15. Kamitani, T., Kito, K., Nguyen, H. P., Wada, H., Fukuda-Kamitani, T., and Yeh, E. T. (1998) *J. Biol. Chem.* **273,** 26675–26682
16. Duprez, E., Saurin, A. J., Desterro, J. M., Lallemand-Breitenbach, V., Howe, K., Boddy, M. N., Solomon, E., de The, H., Hay, R. T., and Freemont, P. S. (1999) *J. Cell Sci.* **112,** 381–393
17. Muller, S., Matunis, M. J., and Dejean, A. (1998) *EMBO J.* **17,** 61–70
18. Zhong, S., Hu, P., Ye, T. Z., Stan, R., Ellis, N. A., and Pandolfi, P. P. (1999) *Oncogene* **56,** 7941–7947
19. Bischof, O., Kirsh, O., Pearson, M., Itahana, K., Pelicci, P. G., and Dejean, A. (2002) *EMBO J.* **13,** 3358–3369
20. Wang, Z. G., Delva, L., Gaboli, M., Rivi, R., Giorgio, M., Cordon-Cardo, C., Grosveld, F., and Pandolfi, P. P. (1998) *Science* **279,** 1547–1551
21. Wang, Z. G., Ruggero, D., Ronchetti, S., Zhong, S., Gaboli, M., Rivi, R., and Pandolfi, P. P. (1998) *Nat. Genet.* **20,** 266–272
22. Fogal, V., Gostissa, M., Sandy, P., Zacchi, P., Sternsdorf, T., Jensen, K., Pandolfi, P. P., Will, H., Schneider, C., and Del Sal, G. (2000) *EMBO J.* **19,** 6185–6195
23. Pearson, M., Carbone, R., Sebastiani, C., Cioce, M., Fagioli, M., Saito, S., Higashimoto, Y., Appella, E., Minucci, S., Pandolfi, P. P., and Pelicci, P. G. (2000) *Nature* **406,** 207–210
24. Ferbeyre, G., de Stanchina, E., Querido, E., Baptiste, N., Prives, C., and Lowe, S. W. (2000) *Genes Dev.* **14,** 2015–2027
25. Momand, J., Zambetti, G. P., Olson, D., George, D., and Levine, A. J. (1992) *Cell* **69,** 1237–1245
26. Oliner, J. D., Kinzler, K. W., Meltzer, P. S., George, D., and Vogelstein, B. (1992) *Nature* **358,** 80–83
27. Haupt, Y., Maya, R., Kazaz, A., and Oren, M. (1997) *Nature* **387,** 296–299
28. Kubbutat, M. H., Jones, S. N., and Vousden, K. H. (1997) *Nature* **387,** 299–303
29. Boyd, S. D., Tsai, K. Y., and Jacks, T. (2000) *Nat. Cell Biol.* **9,** 563–568
30. Geyer, R. K., Yu, Z. K., and Maki, C. G. (2000) *Nat. Cell Biol.* **9,** 569–573
31. Gu, J., Nie, L., Kawai, H., and Yuan, Z. M. (2001) *Cancer Res.* **18,** 6703–6707
32. Kawai, H., Nie, L., Wiederschain, D., and Yuan, Z. M. (2001) *J. Biol. Chem.*

276, 45928–45932
33. Maul, G. G., Negorev, D., Bell, P., and Ishov, A. M. (2000) *J. Struct. Biol.* **129,** 278–287
34. Borden, K. L. B. (2002) *Mol. Cell. Biol.* **22,** 5259–5269
35. Doucas, V., Tini, M., Egan, D. A., and Evans, R. M. (1999) *Proc. Natl. Acad. Sci. U. S. A.* **6,** 2627–2632
36. Pearson, M., and Pelicci, P. G. (2001) *Oncogene* **49,** 7250–7256
37. Zhong, S., Salomoni, P., and Pandolfi, P. P. (2000) *Nat. Cell Biol.* **5,** E85–E90
38. Negorev, D., and Maul, G. G. (2001) *Oncogene* **49,** 7234–7242
39. Zhong, S., Muller, S., Ronchetti, S., Freemont, P. S., Dejean, A., and Pandolfi, P. P. (2000) *Blood* **95,** 2748–2752
40. Lallemand-Breitenbach, V., Zhu, J., Puvion, F., Koken, M., Honore, N., Doubeikovsky, A., Duprez, E., Pandolfi, P. P., Puvion, E., Freemont, P., and de The, H. (2001) *J. Exp. Med.* **193,** 1361–1371
41. Borden, K. L., Campbell Dwyer, E. J., and Salvato, M. S. (1998) *J. Virol.* **72,** 758–766
42. Desbois, C., Rousset, R., Bantignies, F., and Jalinot, P. (1996) *Science* **273,** 951–953
43. Maul, G. G., and Everett, R. D. (1994) *J. Gen. Virol.* **75,** 1223–1233
44. Yu, E., Joo, Y. K., and Lee, I. (1999) *Int. J. Mol. Med.* **3,** 591–596
45. Blondel, D., Regad, T., Poisson, N., Pavie, B., Harper, F., Pandolfi, P. P., de The, H., and Chelbi-Alix, M. K. (2002) *Oncogene* **21,** 7957–7970
46. Regad, T., and Chelbi-Alix, M. K. (2001) *Oncogene* **20,** 7274–7286
47. Chan, H. M., and La Thangue, N. B. (2001) *J. Cell Sci.* **114,** 2363–2373

Physical and Functional Interactions between PML and MDM2

Xiaolong Wei, Zhong Kang Yu, Arivudainambi Ramalingam, Steven R. Grossman, Jiang H. Yu, Donald B. Bloch and Carl G. Maki

J. Biol. Chem. 2003, 278:29288-29297.
doi: 10.1074/jbc.M212215200 originally published online May 19, 2003
